EFFECT OF INLET GEOMETRY ON THE TURBINE BLADE TIP REGION HEAT TRANSFER COEFFICIENT AND EFFECTIVENESS

J. H. Yoon, R. F. Martinez-Botas
Thermofluid Section
Department of Mechanical Engineering
Imperial College of Science, Technology and Medicine
London
England

ABSTRACT

An experimental investigation of the local film cooling effectiveness and heat transfer coefficient downstream of a row of elongated holes in a simulated axial turbine blade tip is presented. Film cooling is needed to protect the turbine blade tip region from high heat transfer rates, especially when cooling by convection is insufficient to keep the temperature distribution of the blade within the limits required. Accurate heat transfer predictions in this region of the blade are particularly difficult given the dimensionality of the flow and the narrow passage typical of turbine blades. The effect of inlet geometry, film cooling injection point, and blowing ratio are examined for an injection on the blade tip itself close to the pressure surface corner. Additionally, the corner radii between the pressure surface and the tip were varied. The experimental method uses the steady state liquid crystal technique. Film cooling injection provides the tip with a blanket of protection from the hot leakage flow. This extends far downstream of the holes at higher blowing ratios. Inlet curvature provides greater local film cooling effectiveness but it lacks streamwise film cooling coverage. It is important to have direct injection onto the separation bubble for greater lateral film cooling coverage.

NOMENCLATURE

b	width of the injection hole
D	channel hydraulic diameter $(\frac{4*CrossSectionalArea}{Wettedperimeter})$
h	heat transfer coefficient (W/m^2K)
H	clearance gap height $(= 24\text{mm})$
HSI	colour space hue,saturation and intensity
M	blowing ratio $(\rho_c U_c/\rho_\infty U_\infty)$
Nu	Nusselt number (hx/κ)
L	distance from inlet to upstream edge of the injection hole
q''	wall heat flux(W/m^2)
r	radius of inlet corner
Re_m	Reynolds number based on hydraulic diameter $(\rho UD/\mu)_\infty$
s	Hole Spacing
T	temperature (K)
x	streamwise coordinate from downstream edge of injection hole
W	Width of the injection hole

Greek Symbols

η	film cooling effectiveness $(T_{aw}-T_\infty)/(T_2-T_\infty)$
κ	thermal conductivity (W/mK)
μ	dynamic viscosity (Ns/m^2)
ν	kinematic viscosity (m^2/s)
ρ	density (kg/m^3)

Subscripts

∞	freestream
c	coolant
aw	adiabatic wall
w	wall

REPORT DOCUMENTATION PAGE

Form Approved OMB No. 0704-0188

PLEASE DO NOT RETURN YOUR FORM TO THE ABOVE ADDRESS.

1. REPORT DATE *(DD-MM-YYYY)*	2. REPORT TYPE	3. DATES COVERED *(From – To)*
05-12-2002	Final Report	17 May 2002 - 17-Aug-02

4. TITLE AND SUBTITLE

Contract Title: Measurements Of Local Heat Transfer Coefficient And Film Cooling Effectiveness In Turbine Cooled Tip Geometries

Final Report title: Effects of Inlet Geometry on the Turbine Blade Tip Region Heat Transfer Coefficient and Effectiveness.

5a. CONTRACT NUMBER
F61775-02-WE003

5b. GRANT NUMBER

5c. PROGRAM ELEMENT NUMBER

6. AUTHOR(S)

Professor Ricardo Fernando Martinez Botas Mateo

5d. PROJECT NUMBER

5d. TASK NUMBER

5e. WORK UNIT NUMBER

7. PERFORMING ORGANIZATION NAME(S) AND ADDRESS(ES)

Imperial College of Science, Technology and Medicine
Exhibition Rd.
London SW7 2BX
United Kingdom

8. PERFORMING ORGANIZATION REPORT NUMBER

N/A

9. SPONSORING/MONITORING AGENCY NAME(S) AND ADDRESS(ES)

EOARD
PSC 802 BOX 14
FPO 09499-0014

10. SPONSOR/MONITOR'S ACRONYM(S)

11. SPONSOR/MONITOR'S REPORT NUMBER(S)
SPC 02-4003

12. DISTRIBUTION/AVAILABILITY STATEMENT

Approved for public release; distribution is unlimited.

13. SUPPLEMENTARY NOTES

14. ABSTRACT

This report results from a contract tasking Imperial College of Science, Technology and Medicine as follows: The project will involve the quantification of the flow and surface characteristics of turbine blade tip cooling geometry with velocity and turbulence distributions relevant to the gas turbine designer. The experimental program will provide measurements of the film cooling adiabatic effectiveness and heat transfer coefficient in a simulated blade tip, with injection from the pressure surface side near the tip. The program will be progressive and interactive, starting with a single row of film cooling holes with injection from the pressure surface side near the tip, moving towards other representative injection configurations: slot injection on the tip surface and groove-tip geometry. The project will supply validation data for the 3D Navier-Stokes solver Glenn-HT, currently used by NASA, and it will also provide insight into the performance of advanced cooling geometry configurations.

The experiments will make use of liquid crystal thermography to obtain the heat transfer data. The data acquisition method corresponds to the steady-state technique with the use of wide band liquid crystals. It requires a reduced number of experiments when compared with narrow band crystals and thermocouples, and provides a high degree of spatial resolution and reduced uncertainty level. It will be accompanied by data from small-diameter thermocouples, hot wires and pressure transducers.

It is proposed to extend this program to include the effect of two variables: ratio of hole diameter/duct height and axial location of the injection holes. These have been identified from the completed part of the program as critical and not investigated before in detail. Furthermore it is proposed to look at the fluid dynamics of the flow in the tip corner to identify the separation bubble location and reattachment.

15. SUBJECT TERMS

EOARD, Gas Turbines, Turbine Blade Cooling

16. SECURITY CLASSIFICATION OF:			17. LIMITATION OF ABSTRACT	18, NUMBER OF PAGES	19a. NAME OF RESPONSIBLE PERSON
a. REPORT	b. ABSTRACT	c. THIS PAGE			Wayne Donaldson
UNCLAS	UNCLAS	UNCLAS	UL		19b. TELEPHONE NUMBER *(Include area code)* +44 (0)20 7514 4299

From: Romine, David [david.romine@london.af.mil]
Sent: Thursday, February 06, 2003 7:31 AM
To: lfenster@DTIC.MIL
Subject: FW: SPC-02-4003 Final Report
What Wayne is trying to say below is to use the title from the SF298 as this is what he contracted for.

Dave
-----Original Message-----
From: Donaldson, Wayne
Sent: 06 February 2003 12:25
To: Romine, David
Subject: RE: SPC-02-4003 Final Report

Good Save,
I've added both to the 298. The contract title should be used if you have to pick one.
Thanks!
Wayne

> -----Original Message-----
> **From:** Romine, David
> **Sent:** 05 February 2003 12:36
> **To:** Donaldson, Wayne
> **Subject:** FW: SPC-02-4003 Final Report
>
> She's right. which one is correct?
>
> Dave
> -----Original Message-----
> **From:** Fenster, Lynn [mailto:lfenster@DTIC.MIL]
> **Sent:** 05 February 2003 12:34
> **To:** Romine, David
> **Subject:** RE: SPC-02-4003 Final Report
>
> David,
> Title on document and on 298 are not the same. Which one is correct?
> Lynn
>
> -----Original Message-----
> From: Romine, David [mailto:david.romine@london.af.mil]
> Sent: Wednesday, February 05, 2003 5:32 AM
> To: Delorie, Rusty; Fenster, Lynn
> Subject: SPC-02-4003 Final Report
>
> <<finalreport.pdf>> <<SF298.doc>>
> > -----Original Message-----
> > From: Donaldson, Wayne
> > Sent: 04 February 2003 10:49
> > To: Romine, David
> > Subject: SPC 024003 DTIC Submission Request
> >
> > Please prepare the Final Deliverable of SPC 024003 and submit to DTIC.
> >
> > See FINAL REPORT in DOCS folder.

>
> Thanks!

INTRODUCTION

The desire for higher efficiency and specific thrust in gas turbine systems has led to an increased interest in the heat transfer aspects of gas turbine components. An increase in turbine entry temperature is required to achieve these objectives. Turbine inlet temperature has almost doubled over the past 25 years. However, this means gas turbine components are exposed to adverse thermal environments; the temperature of the turbine blade material may exceed its limits and so it has to be protected from hot gases with effective cooling systems. A direct result of this has been an improvement in blade cooling methods and the development of temperature-resistant materials. Detailed attention to the turbine blade cooling technology of the gas turbine engine is required for further improvements in engine performance and durability. The cooling air used is taken from the engine compressor's later stages; this extraction of high-pressure air has a negative effect on the overall thermal efficiency. The minimization of cooling air used is another important motivation for the development of an improved prediction method for the estimation of convection heat transfer in turbine blades.

One of the most problematic areas in gas turbine engines is the blade tip region, especially near the trailing edge, where it is very difficult to cool it sufficiently. In all configurations with unshrouded tips, a clearance gap exists between the turbine blade and the outer shroud.

The pressure difference between the suction and pressure sides of the turbine blade drives a sink-like flow through the gap. This is generally known as tip leakage flow. It is composed of both mainstream fluid from the hot gas path region near the blade tip and cooler fluid from the blade pressure surface also near the tip. This combination of fluids entering the clearance gap induces high convective heat transfer coefficients on the blade tip surface. The resultant thermal loading can be significant and detrimental to the turbine blade tip durability, leading to early failure. A widening of the clearance gap due to significant oxidation and material weight loss can rapidly occur, thus increasing leakage flow loss.

A typical clearance gap flow is illustrated in Fig. 1, where the arrows represent the motion of the gas close to the tip of the blade. The tip width between the pressure and suction side varies along the blade-chord. The flow path length can be up to 20 times the gap height over the widest part of the turbine blade tip. It is thus possible to derive an experimental representation of this wide region in a simplified wind tunnel experiment.

Literature Survey

The methodology for predicting and minimizing tip leakage flows was developed with the help of a water table cascade rig by Booth et al.(1982), who showed that the tip leakage flow is predominantly an inviscid phenomena. The normal velocity component of the blade tip leakage flow was treated in terms

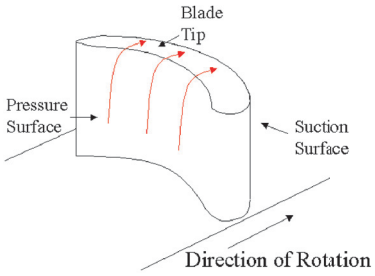

Figure 1. Clearance tip leakage flow

of discharge coefficient; a simple discharge experiment with a cascade model was adopted to investigate tip leakage configurations. Bindon (1986) measured tip clearance flow for the leading to trailing edge of a linear turbine cascade model and identified and quantified loss mechanisms. Simple flow visualization techniques showed details of the flow structure in and around the tip clearance region. Mixing, internal shear flow and secondary flows were identified and discussed. Sjolander and Cao (1995) conducted similar experimental measurement in a single idealized, large-scale tip gap model; with this larger scale it was possible to obtain more detailed measurement inside the clearance gap. In both cases, the sharp corner at the entrance of the gap induced a separation bubble in the early portion of the clearance gap.

Attention has focused on the heat transfer aspect of the tip leakage flows. Heat transfer rates on the tip of the blade have been determined in various studies and the results indicate that these are some of the highest found in turbine components. Experimental and numerical investigations of local convective heat transfer at the tip region with varying tip geometry have been conducted by various researchers. Metzger and Rued (1989) investigated the influence of tip leakage flow on heat transfer and flow development along the pressure side of the turbine blade. The clearance flow field measurements were conducted with a laser-doppler anemometer to aid interpretation of the heat transfer results and very high velocities and accelerations were generated very near the clearance gap. Chyu et al. (1989) used the naphthalene sublimation technique to determine detailed heat transfer characteristics. The heat transfer coefficient was strongly influenced by the geometry of the blade tip. Mayle and Metzger (1982) studied the relative motion between a flat blade tip and stationary shroud and showed that the relative motion did not have a significant effect on the averaged convection tip heat transfer coefficient for a flat tip model. Chyu et al. (1987) introduced a grooved turbine blade tip geometry to decrease the pressure difference between the suction and the pressure side of the blade, thus reducing the clearance gap flow. The effect of shroud motion was confined to a thin layer adjacent to the shroud in both cases. The cavity region flow patterns,

mean velocity profiles and heat transfer coefficient are virtually independent of relative motion.

Most of the published work concentrates on clearance gap flows but not on the associated tip cooling system. There are only limited published experimental and computational data on film cooling injection for simulated turbine blade tips. Kim and Metzger (1995) and Kim et al. (1995) measured heat transfer and film effectiveness for various combinations of clearance gap heights, Reynolds number and blowing ratio with different injection geometries using a transient thermal liquid crystal technique. The data shows strong dependency of film cooling performance on the shape of the coolant supply holes and the injection locations for a given tip geometry.

In terms of numerical work, Chen et al. (1993) used a two-dimensional Navier-Stokes equation model to simulate the effect of tip flow for flat and squealer types of blade tips. This was compared with experimental measurement. The results showed that secondary injection into the tip gap leads to a reduction of the total mass flow entering the gap. However, the two-dimensional simulation imposed severe limitations on the range of geometries that could be studied. Ameri and Ridgby (1999) used a three-dimensional Reynolds-averaged Navier-stokes solver to predict the rate of tip heat transfer and film cooling effectiveness on a simulated blade tip and provided numerical flow visualization of the cooling fluid distribution on the clearance gap. The heat transfer prediction was dependent on grid resolutions.

EXPERIMENTAL APPARATUS

Measurement Technique The experimental method used in this study is based on the steady-state heat transfer technique. This method can obtain both heat transfer coefficient and effectiveness values by either employing a constant heat flux surface or a nominally adiabatic surface.

Typical steady state experiments involve an electrically heated constant heat flux surface with a cold mainstream and heated secondary injection, thus giving film heating; the reverse would provide film cooling (i.e. hot main stream and cold secondary injection). The heat transfer coefficient should be independent of the temperature difference for a constant property flow. The heat transfer coefficient is commonly defined as:

$$h = \frac{q''}{(T_w - T_{aw})} \tag{1}$$

The heat transfer coefficient can also be defined as in Eqn. 2 when the injection and freestream are at the same temperature, Eriksen (1971).

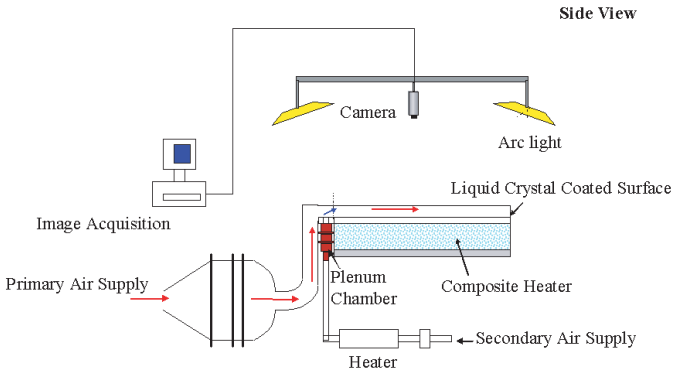

Figure 2. Experimental set-up

$$h = \frac{q''}{(T_w - T_\infty)} \tag{2}$$

In the case of an unheated injection, where the injection flow temperature is equal to the mainstream temperature, the mainstream recovery temperature is used as the adiabatic wall temperature. For heated injection, the adiabatic wall temperature has to be measured on an adiabatic test surface (i.e $q'' = 0$) in a separate experiment using an unheated wall.

The film cooling effectiveness (η) is defined in Eqn. (3) for a low speed and a constant property flow.

$$\eta = \frac{(T_{aw} - T_\infty)}{(T_c - T_\infty)} \tag{3}$$

Application of Thermographic Liquid Crystals The reflected light from liquid crystals is dependent on the spectral intensity of the incident light and contains a peak whose wavelength depends on the given temperature. The relationship between the RGB data and temperature is not simple since the RGB signal is dependent on the local illumination strength. The most appropriate format is HSI (hue, saturation and intensity). Hue describes colour; saturation measures the degree to which a pure colour is diluted with white; and intensity is a colour-neutral attribute that describes brightness. Hue gives a simple and monotonic indication of the wavelength of the colour signal. Camci at al. (1992) suggest that hue alone can be used to represent temperature dependent behaviour of a liquid crystal. Hue value is independent of the local illumination strength and has a direct relationship to the local temperature.

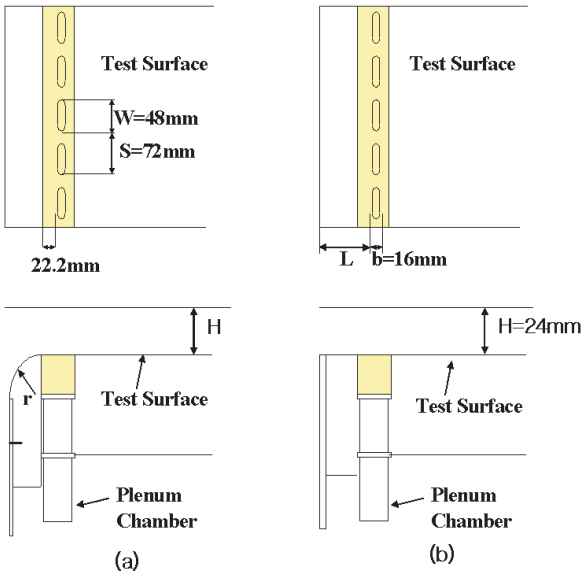

Figure 3. Experimental set-up

r	r/H	L	L/H
r0	-	L0	1
r1	1	L1	2
r2	1.5	L2	2.4
r3	2	L3	3

Table 1. Tip Geometry Dimension.

The Injection System and Plenum chamber The experimental set up is shown in Fig. 2. The air injectant or secondary air was supplied from filtered laboratory compressor air. The flow was then passed through an inline pipe heater, followed by a plenum chamber that supplied the injection plate. A flow straightener was inserted upstream of the rotameter to achieve uniform flow.

For a heat injection experiment, a 1890W in-line heater, controlled by a variac, was adjusted to provide a heated jet at $40^{\circ}C \pm 0.1^{\circ}C$. The temperature difference between free stream and jet was under $20^{\circ}C$; this small difference is important to satisfy the constant property flow assumption. The free stream temperature was measured with a thermocouple in the inlet corner section before the free stream flow mix with the film coolant. The injectant temperature was measured with a thermocouple located in a hole at a depth equivalent to 2 diameters. A narrow plenum chamber with three fine gauze screens was connected to the outlet of an inline pipe heater. The plenum chamber was designed to smooth out any velocity non-uniformity. The uniformity test showed a maximum non-uniformity of $\pm 5\%$ in the distribution across the injection holes.

The cross section and plane views of the injection geometry is shown in Fig. 3. The test plate had a row of five elongated holes at 90° to the test surface in the streamwise direction. The holes were arranged so that the central hole lay on the centreline of the test plate on which the liquid crystals were painted. This space is limited by the plenum chambers underneath the injection plate. The reason for multiple holes was to ensure the fluid dynamical environment which simulates the jet interaction present in three dimensional film cooling situations. An additional section was inserted in front of the injection plate to vary the film cooling injection point or the corner radius between the pressure surface and tip while a constant value of H were maintained. The dimensions of the injection plates and sections are shown in Table 1. The measurement area was concentrated in the vicinity of the central hole where side-wall effects are negligible.

Constant Heat Flux Test Surface A 360mm by 1000mm composite test plate was designed to produce a constant heat flux with a minimum lateral conduction across the plate. The constant heat composite consisted of 0.2mm thick stainless steel sheet which was heated with 18 Inconnel strips covering the entire width of the test surface. The heating elements, each 54mm in width, were connected to the electrical power supply by a series of 3mm thick copper bus bars on each end of the test plates.

Rastogi (1972) applied electrical current directly to the stainless steel test surface but this technique requires a large current and is prone to non uniform heat flux distribution. Like Ericksen (1971), the current experiment used serpentine Inconnel strips without silicon impregnated sheet. A 0.2mm thick silicon impregnated sheet was placed in between the stainless steel sheet and the Inconnel heater strip. This provided electrical insulation and promoted heat conduction to the test surface so as to improve the uniformity of heat flux distribution.

The microencapsulated liquid crystal used in the current study was supplied by Thermax with a bandwidth of 10°C. The test plate received only incident light emitted from the arc light and eliminated variations in illumination. The shield also protected the liquid crystal surface form UV radiation damage. A Hoya polarising filter was installed onto the camera lens to minimize reflections from the perspex roof.

A single phase transformer with two 25 volts r.m.s secondary windings operating at 35 amperes was made to power the heating elements. The uniformity of the resistance of the Inconnel strips was checked by measuring voltage across a given distance before the layer of stainless sheet was mounted. Further assessment of the uniformity of heat flux was carried out with the liquid crystal coating. At a given electrical setting and operating conditions, the standard deviation of surface temperature

was 0.2°C over the entire test plate. Adiabatic wall temperatures were determined by operating the set up with injection of the heated secondary air and no heat flux from the test surface. In all cases, the primary flow, the secondary flow and the wall heat flux was set for each set of given operating conditions and run for half an hour in order for the experimental set up to come to a steady-state.

Data Acquisition and Processing Images were captured by a JVC colour CCD camera (TK-885E) ,positioned directly over the test plate, which was controlled by a 24-bit frame grabber. The images were captured and stored as a three-dimensional matrix of red, green and blue (RGB) values. Code was written to control the capture rate, and the sequence of images was stored on hard disk for post-processing. The RGB images were first converted to HSI colour space using commercial software, and then split into separate pictures of hue, saturation and intensity. Frame averaging and smoothing were applied to reduce salt and pepper noise signals without any loss of information, [Babinsky and Edwards (1996), Farina et al. (1993) and Lee and Yianneskis (1993)]. A 3 x 3 spatial median filter was then used to remove any isolated pixels due to imperfections in the liquid crystal layer. Image processing began by importing hue-only images for the test plate and the hue-temperature calibration curve were used to convert hue matrix values to temperature. A code was written to calculate heat transfer coefficient and film cooling effectiveness from temperature matrix values.

Uncertainty Analysis Uncertainties are evaluated by the method of Kline and McClintock (1953). Corrections are applied to consider heat loss through thermocouple leads using the method proposed by Schneider (1974). Corrections for radiation from the heated test surface coated with liquid crystals and conduction out the back of the test surface are included into the analysis, such that subtraction of these corrections from the average heat generated within the heater gives the net local heat flux. The uncertainty in h is approximately $\pm$7% and the uncertainty in effectiveness is approximately $\pm$9% respectively

RESULTS AND DISCUSSION

The section is divided into two parts: the first deals with film cooling effectiveness and the second with heat transfer coefficient measurement.

The Reynolds number and blowing ratio was based on the clearance gap hydraulic diameter for the main flow. Measurement from the central section of the test plate with one periodic width was used to obtain the laterally-averaged values.

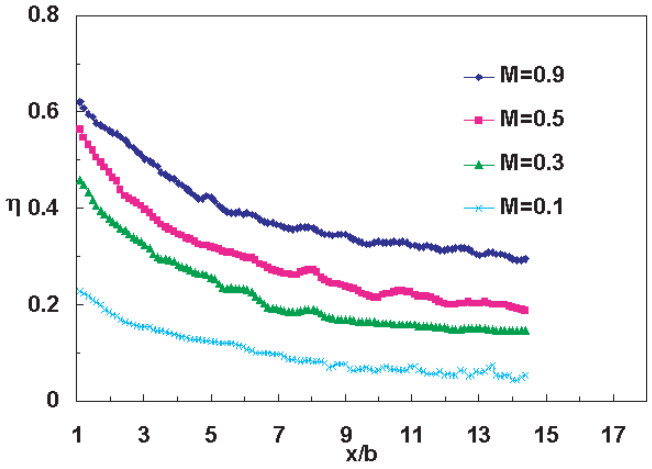

Figure 4. Laterally Averaged Effectiveness Re_m=30,000 L=L0 r=r0

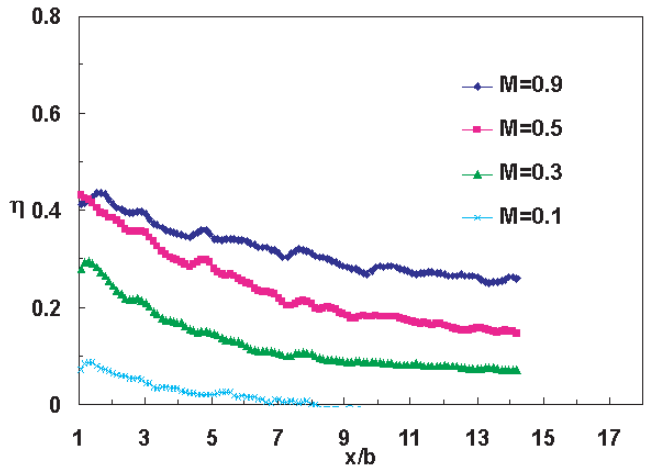

Figure 5. Laterally Averaged Effectiveness Re_m=30,000 L=L1 r=r0

Film Cooling Effectiveness

Effect of Injection Point on Film Cooling Effectiveness Fig. 4 illustrates the effect of increasing the blowing ratio on the laterally-averaged effectiveness values with Re_m=30,000 and L=L0. These are consistent with the results of Yuen (2000); the film cooling effectiveness varies from a value of near unity at the point of injection to zero far downstream, where the secondary flow is diluted and the adiabatic wall temperature approaches the free stream value. In the case of flat plate film cooling, there is an optimum blowing ratio due to the fact that there is lift-off of coolant from the boundary layer around M=0.4$\sim$0.6. In the case of the sharp corner clearance gap cooling, geometrical restriction and presence of the separation bubble constrains the early development of lift-off. The expansion of the

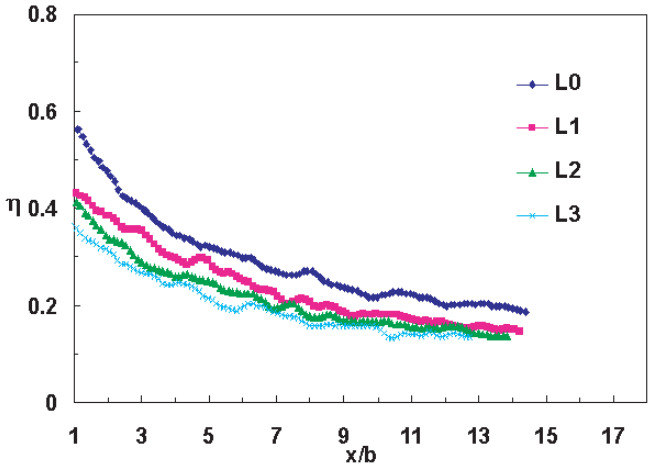

Figure 6. Laterally Averaged Effectiveness Re_m=30,000 M=0.5 r=r0

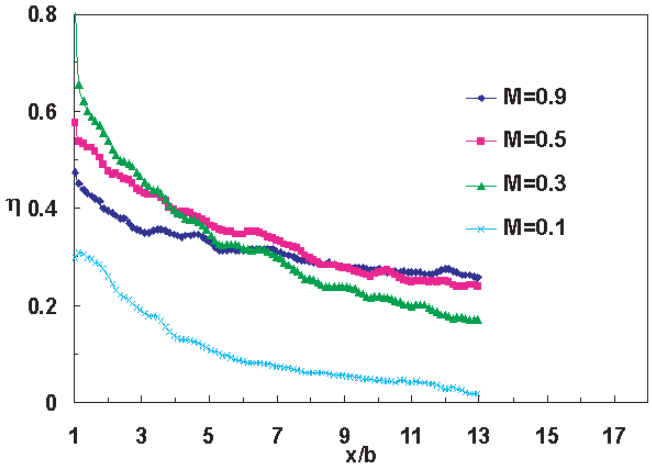

Figure 8. Laterally Averaged Effectiveness Re_m=30,000 L=L0 r=r3

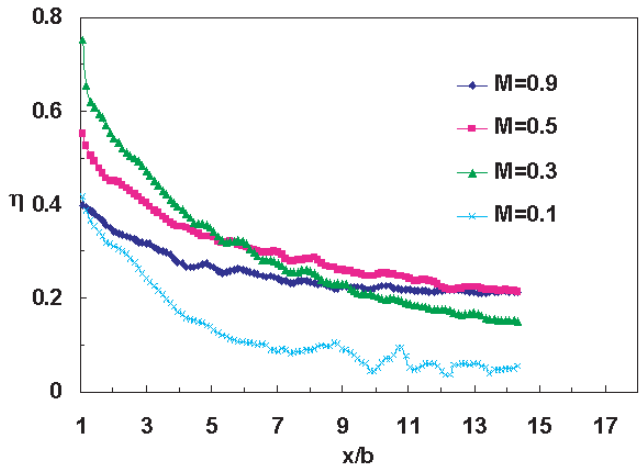

Figure 7. Laterally Averaged Effectiveness Re_m=30,000 L=L0 r=r1

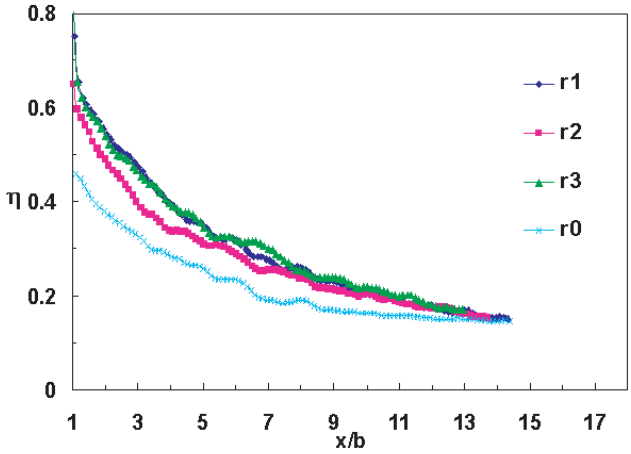

Figure 9. Laterally Averaged Effectiveness Re_m=30,000 L=L0 M=0.3

coolant into the freestream, is restricted so no optimum is found. The laterally-averaged effectiveness increases monotonically at higher blowing ratios.

In blade tip cooling, the film cooling effectiveness does not approach to zero far downstream. The contribution to the freestream from film coolant is substantial in this case; hence it has greater influence on the freestream temperature.

Fig. 5 shows the effects of injection at the point of L1. Lower effectiveness values compared to the L=L0 case were found in all blowing ratios. Increasing in blowing ratio from M=0.5 to M=0.9 did not significantly increase overall effectiveness level compared to the level of increase from M=0.3 to M=0.5.

The turbine blade generally has a sharp corner at the entrance of the gap which induces separation bubble formation on the pressure side. The presence of a separation bubble on the blade tip was examined by Bindon (1986) and Sjolander and Cao (1995). Moore and Tilton (1988) showed that gap flow was essentially loss-free up to the separation bubble and then underwent sudden expansion causing significant diffusion and mixing. Heyes et al. (1993) suggested that the mixing would start immediately downstream of the separation bubble at the 1.5 gap height distance away from the pressure side corner and be completed when the streamwise distance exceeded six times the gap height. Fig. 6 summarizes the effect of different injection points with Re_m=30,000 and M=0.5. The laterally-averaged effectiveness decreases as the injection point moves away from the pressure side edge. The injection point Lo represent a direct film cooling injection to the separation bubble. L1, L2, and L3 correspond to

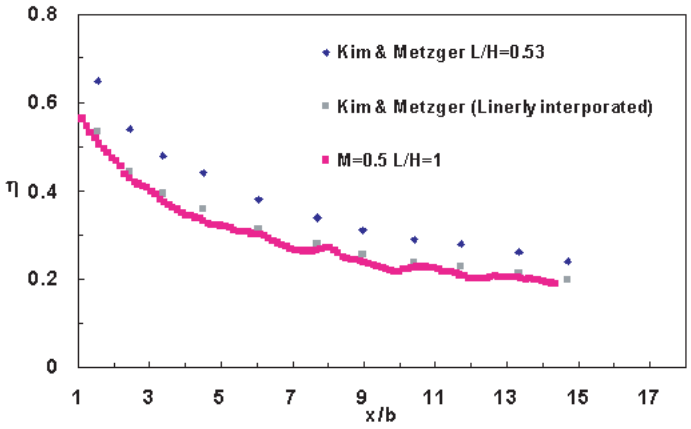

Figure 10. Laterally Averaged Effectiveness Re_m=30,000 M=0.5 r=r0

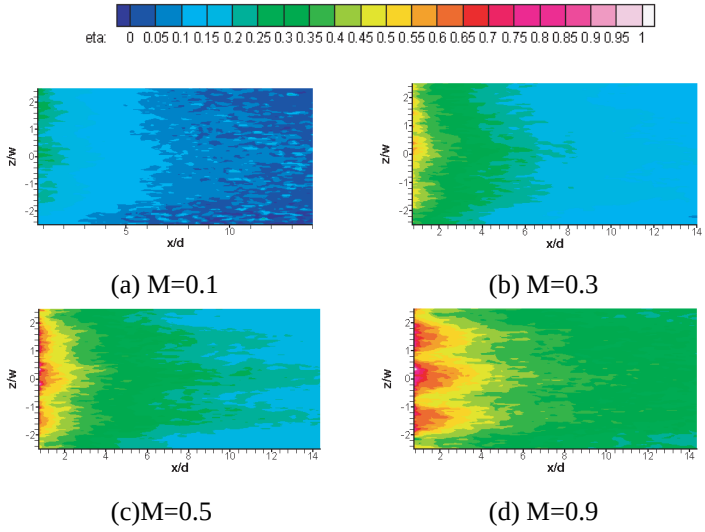

(a) M=0.1 (b) M=0.3

(c)M=0.5 (d) M=0.9

Figure 11. Film Cooling Effectiveness Re_m=30,000 L=L0 r=r0

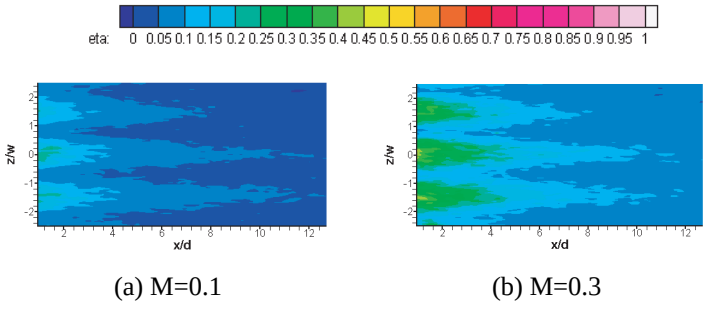

(a) M=0.1 (b) M=0.3

(c)M=0.5 (d) M=0.9

Figure 12. Film Cooling Effectiveness Re_m=30,000 L=L3 r=r0

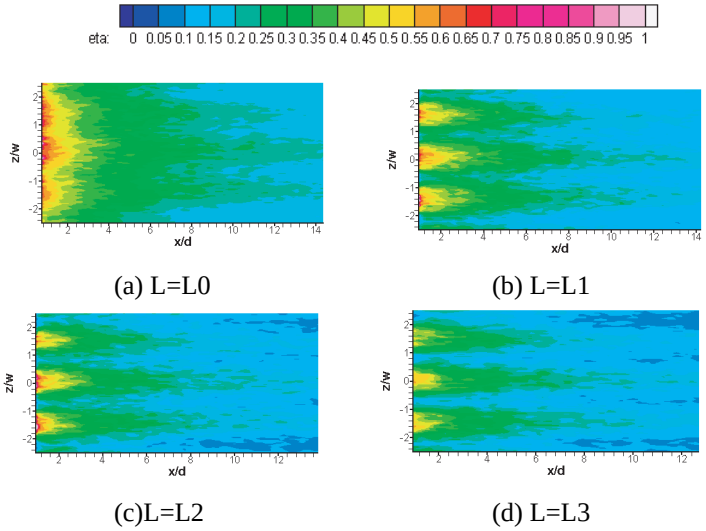

(a) L=L0 (b) L=L1

(c)L=L2 (d) L=L3

Figure 13. Film Cooling Effectiveness Re_m=30,000 M=0.5 r=r0

injection into the subsequent mixing region. It is therefore reasonable to assume that moving away from the separation bubble reduced the interaction of freestream and film coolant.

Effect of Inlet Geometry on Film Cooling Effectiveness Fig. 7 and 8 show the effect of the curved pressure side corner. In contrast to a sharp corner, there is an optimum blowing ratio due to the lift-off of coolant from the boundary layer at M=0.3 for all curved corners. The inlet radius is key factor in both the formation the separation bubble and its size. Fig. 9 indicates that the radius of the pressure side corner at lower blowing ratios induce higher laterally averaged film cooling than the sharp edge case of L0. However, changing the radius seems to have very little effect on the effectiveness which suggests that the separation bubble was eliminated in all cases. Also the sink-like flow characteristics near the pressure side give rise to high velocities and accelerations into the clearance gap which cause thinning of the boundary layer in all three radii.

Fig. 10 includes the effectiveness level of Kim and Metzger (1995) and they are approximately 20% larger than those obtained in this study. The L/H value of Kim and Metzger (L/H=0.53) is almost half of the lowest value of L/H in the present experimental set-up (L/H=1). It is found in the current study and presented in Fig. 6 that the effectiveness values decrease as L/H increases. Therefore, the agreement between Kim and Metzger's data and the current study is reasonable. Furthermore, this graph also shows linearly interpolated data of Kim and Metzger which is in very close agreement with M=0.5 L/H=1

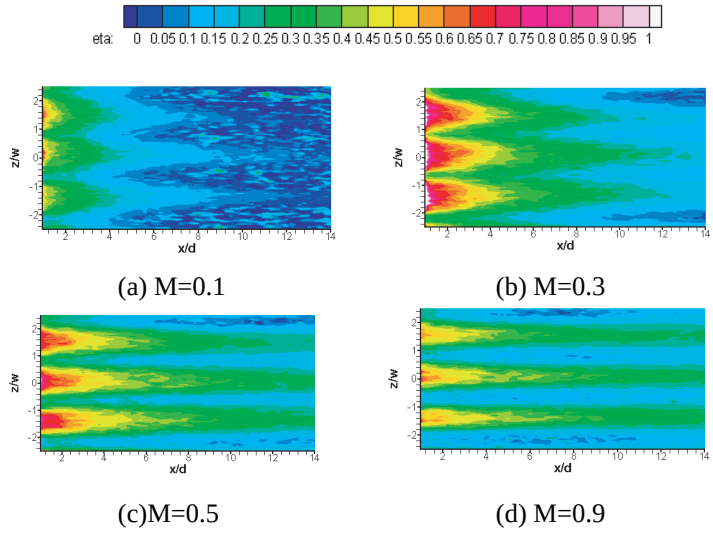

Figure 14. Film Cooling Effectiveness Re_m=30,000 L=L0 r=r1

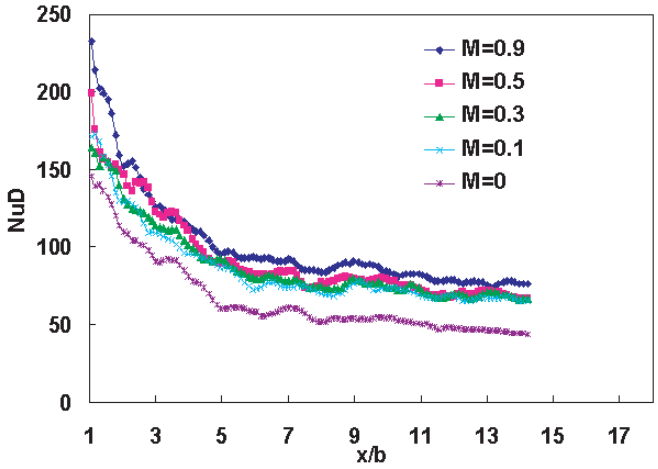

Figure 15. Laterally Averaged Nu Re_m=30,000 L=L0 r=r0

case.

Fig. 11 shows the contour plot of variations in the film cooling effectiveness with L=L0. The symmetry in the results is noticeable. At the streamwise location closest to film cooling injection, effectiveness values of near unity are recorded, in the case of the higher coolant blowing ratio of M=0.5 and above [see Fig. 11(C) (D)]. The location of injection holes are clearly shown in the data. The effectiveness values are higher at the centre of the hole and drop considerably in between injection holes. The minimum η value of around 0.4 is still observed even at the mid-point between the injection holes at the higher blowing ratio of M=0.5 and above. In the current set-up, the close chordwise spacing of the holes prevents any zero effectiveness regions between the holes ensuring a good coverage of film cooling flow. However, Fig. 12 shows different results. The effectiveness value is considerably lower in the most of the area and also it lacks film cooling coverage in between injection holes. Fig. 13 clearly demonstrates the effect of coolant injection moving away from the pressure side edge.

Fig. 14 presents different results from the L0 case. The effectiveness value in the vicinity of the hole is considerably higher than the L0 case but it clearly shows the lack of film cooling coverage in between injection holes at given blowing ratios. This again indicates that rounding of the pressure side corner affects the formation of a separation bubble on the blade tip and hence interaction of film coolant and freestream.

The chordwise variations in effectiveness were used to establish the magnitude of local blade tip temperature gradients and hence the amount of the thermal stresses. Chordwise variations of effectiveness tend to be greatest at the highest blowing ratio and the measured effectiveness decreases monotonically in the downstream direction.

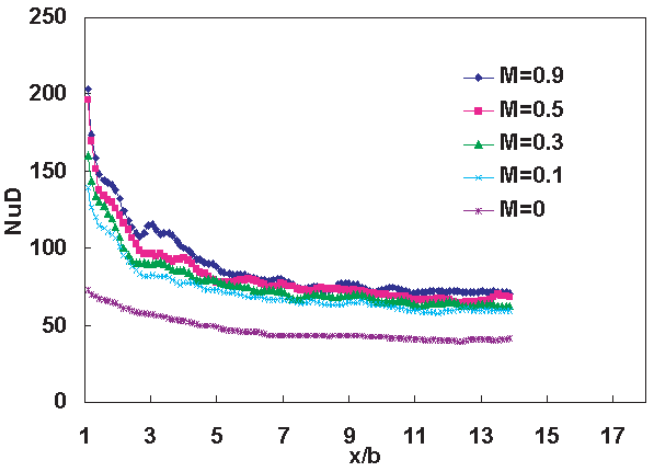

Figure 16. Laterally Averaged Nu Re_m=30,000 r=r1

Heat Transfer Coefficient

Effect of Blowing Ratio on Nusselt number Fig. 15 displays the measured effect of increasing the blowing ratios on the laterally-averaged heat transfer coefficient with Re_m=30,000 and L=L0, presented in the laterally averaged Nusselt number form. The Nusselt number is much higher at the holes nearest the point of injection, reaching close to 200 and dropping to around 80 in the far downstream case for M=0.9. In the lower blowing ratio, the Nusselt number profile is much flatter and has a lower maximum value. Fig. 16 with Re_m=30,000 and r=r1 also shows a similar trend. The effect of blowing ratio on Nusselt number in the tip clearance region is different from conventional film cooling. The important effect in this case is the general tendency for a small increase in Nusselt number over nearly all of the pro-

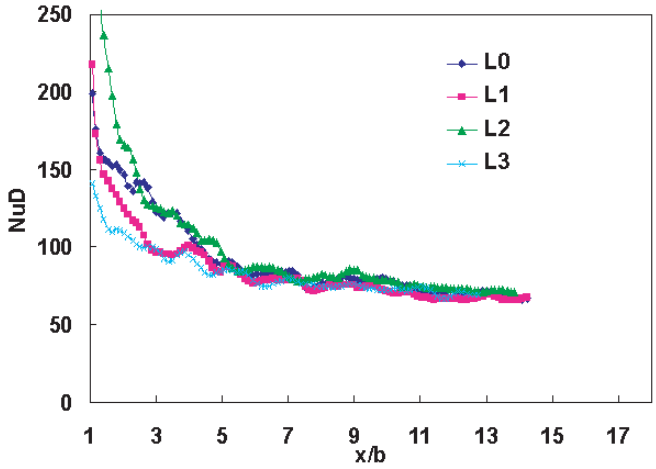

Figure 17. Laterally Averaged Nu Re_m=30,000 M=0.5 r=r0

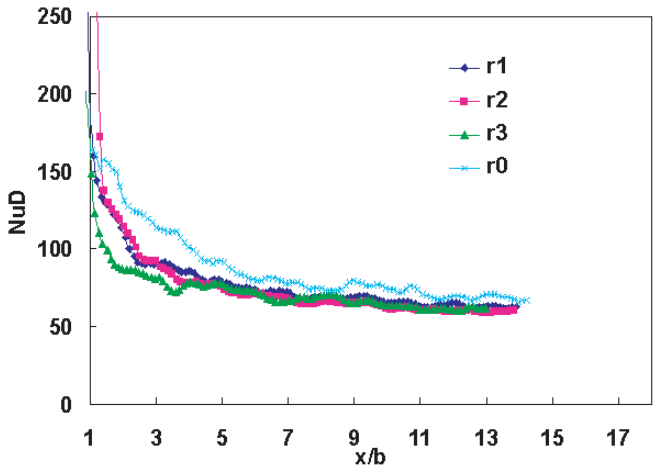

Figure 18. Laterally Averaged Nu Re_m=30,000 M=0.3 L=L0

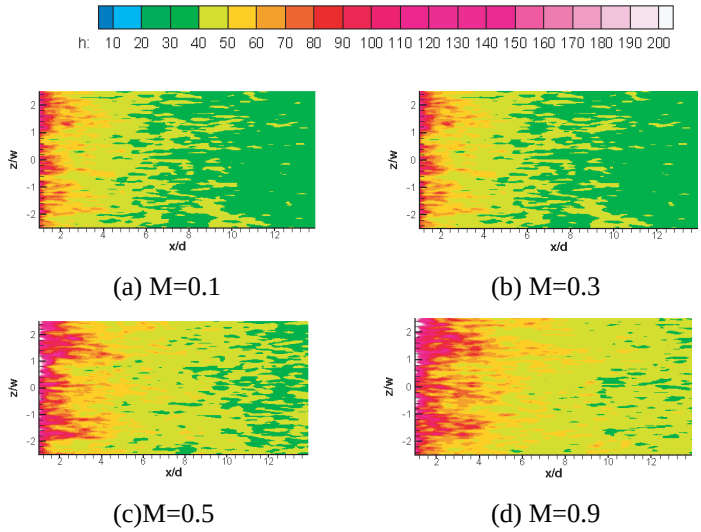

Figure 19. Heat Transfer Coefficient Re_m=30,000 L=L0 r=r1

tected surface with increasing blowing ratio. At higher blowing ratios, more coolant is injected into the boundary layer which in turn acts as a bigger heat sink;there also is an increase in the free stream velocity due to film cooling injection. This is particularly the case in the narrow passage of the clearance gap, where the injection hole width is substantial compared to the clearance gap height. The effect would be insignificant in a wide passage, commonly used in film cooling studies. Fig. 17 presents the effects of film cooling injection point on Nusselt Number. There are small variations of the Nusselt number close to the test span but other cases Nusselt number approaches around 70 in the far downstream region.

Fig. 18 indicates that radius of the pressure side corner at blowing ratios of M=0.3 produced lower Nusselt number than the sharp edge case of L0. However, changing the radius seems to have very little effect on the Nusselt number, which is in line with the earlier effectiveness measurements. The inlet radius affect the formation of the separation bubble, and the acceleration of the tip gap flow cause thinning of boundary layer. That boundary layer is not subsequently affected by changes in the inlet radius.

Film cooling injection produces the highest heat transfer coefficient immediately downstream of the injection holes. However, the surface is still cooler at this point than further down in the stream direction since the film cooling injectant is at a lower temperature than the mainstream. The temperature difference between the surrounding fluid and the clearance gap is smaller then without film cooling. This increase in the peak value near the injection hole due to injection provides a useful parameter for predicting the blade tip thermal loading. The temperature of film injection needs to be low enough to prevent an overall increase in thermal loading on the tip.

Chordwise Variation of Heat Transfer Coefficient

The heat transfer coefficient is evaluated from changes in the adiabatic temperature and wall temperature at a given heat flux. Both of these have a similar chordwise profile, meaning that the overall variation of heat transfer coefficient across the test span is small when compared to the variation of the effectiveness.

Fig. 19 shows variations of convection coefficients along the chordwise direction in the case with Re_m=30,000, r=r1. The local variation for M=0.1 is very small, of the order of $\pm$5 percent, while the variation for M=0.9 is around $\pm$20 percent at the streamwise location closest to the holes but decreases rapidly downstream.

The small chordwise variation supports the idea that the heat transfer coefficients are dominated by the channel entrance effect

at lower blowing ratios, and are only elevated significantly by injection at the higher values.

Conclusion

An experimental investigation of film cooling of a turbine blade tip was conducted. The effect of Reynolds number and blowing ratio was examined in the case of injection on to the blade tip itself close to the pressure surface corner.

Wide band liquid crystal thermography was used. This is capable of mapping the temperature of the whole surface, from which the effectiveness and heat transfer coefficients can be found.

Film cooling injection, with a single row of elongated holes nearest to the pressure side corner, protects the tip from the hot leakage flow though the clearance gap and this extends far downstream of the holes at higher blowing ratios. Inlet curvature gives greater local film cooling effectiveness near the hole but not uniform in the streamwise direction. It is important to have direct injection onto the separation bubble for greater lateral film cooling coverage.

Film cooling injection generally increases the effectiveness value but also increases the convection coefficients. If the film cooling injection temperature is not sufficiently low relative to the clearance leakage flow, injection can lead to an increase in thermal loading on the blade tip. A contour plot of film cooling effectiveness and heat transfer coefficient provides a clear graphical representations of their distribution over a surface.

ACKNOWLEDGMENT

This work was carried out under contract F61775-99-WE095 from the European Office of Aerospace Research and Development (US Air Force); technical coordinators for this effort are C.Raffoul, W.Donaldson and R.Rivir.

REFERENCES

Ameri, A.A., Rigby, D.L. (1999). Analysis of supersonic stall bending flutter in axial-flow compressor by actuator disk theory. Technical Paper 1999-209165, NASA. The 14th International Symposium on Air Breathing Engines, Florence, Italy.

Babinsky, H., Edwards, J.A. (1996). Automatic liquid crystal thermography for transient heat transfer measurements in hypersonic flow. *Experiments in Fluids 21*, 227–236.

Bindon, J.P. (1986). Visualization of axial turbine tip clearance using a linear cascade. Cued/a-turbo tr122 whittle labratory, Cambridge University.

Booth, T.C., Dodge, P.R., Hepworth, H.K. (1982). Rotor-tip leakage:part1-basic methodogy. *ASME Journal of Engineering for power 104*, 154–161.

Camci, C., Kim, K., Hippensteele, S.A. (1992). A new hue capturing technique for the quantitative interpretaion of liquid crystal images used in convective heat transfer studies. *ASME Journal of Turbomachinery 114*, 765–775.

Chen, G., Dawes, W.N., Hodson, H.P. (1993). A numerical and experimental investigaion of turbine tip gap flow. *AIAA 93-2253*.

Chyu, M.K., Metzger, D.E., Hwan, C.L. (1987). Heat transfer in shrouded rectangular cavities. *Journal of Thermophysics and Heat Transfer 1*, 247–252.

Chyu, M.K., Moon, H.K., and Metzger, D.E. (1989). Heat transfer in the tip region of grooved turbine blades. *Journal of Turbomachinery 111*, 131–138.

Eriksen, V.L. (1971). *Film Cooling Effectiveness and Heat Transfer with Injection Through Holes*. Ph. D. thesis, Universiy of Minnesota.

Farina, D.J., Hacker, J.M., Moffat, R.J., Eaton, J.K. (1993). Illuminant invariant calibration of thermochromic liquid crystals. *Visualisation of Heat Transfer Processes ASME 253*, 1–11.

Heyes, F.J.G., Hodson, H.P., and Dailey, G.M. (1993). Measurement and prediction of tip clearance on the tip leakage flow in axial turbine cascade. *ASME Journal of Turbomachinery 115*, 643–651.

Kim, Y.W., Downs, J.P., Soechting, F.O., Abdel-Messeh, W., Steuber, G.D., Tanrikut, S. (1995). A summary of the cooled turbine blade tip heat transfer and film effectiveness investigations. *ASME Journal of Turbomachinery 117*, 1–11.

Kim, Y.W., Metzger, D.E. (1995). Heat transfer and effectiveness on film cooled turbine blade tip models. *ASME Journal of Turbomachinery 117*, 12–21.

Kline, S.J., Mcklintock, F.A. (1953). Describing uncertainties in single sample experiments. *Mechanical Engineering January*, 3–8.

Lee, K.C., Yianneskis, M. (1993). An image processing technique for the analysis of thermotic distribution utilising liquid crystals. Imaging in Transport Processes.

Mayle, R.E., Metzger, D.E. (1982). Heat transfer at the tip of an unshrouded turbine blade. Proc. 7th Intl. Heat Conf. Washington, D.C.

Metzger, D.E., Rued, K. (1989). The influence of turbine clearnce gap leakage on passage velocity and heat transfer near blade tips:part 1-sink flow effects on blade pressure side. *ASME Journal of Turbomachinery 1011*, 284–292.

Moore, J., and Tilton, J.S. (1988). Flow and heat transfer in turbine tip gaps. *ASME Journal of Turbomachinery 111*, 301–309.

Rastogi, A.K. (1972). *Effectivness and Heat Transfer of Three-Dimensional Film Cooling Slots*. Ph. D. thesis, Imperial College of Science, Technology and Medicine, London.

Schneider, P.J. (1974). *Conduction Heat Transfer*. Addison-Wesley, Reading, Mass.

Sjolander, S.A. and Cao, D. (1995). Meaurement of the flow in an idealized turbine tip gap. *ASME Journal of Turbomachinery 117*, 578–584.

Yuen, C.H.N. (2000). *Measurement of Local Heat Transfer Coefficient and Film Cooling Effectiveness in Film Cooling Geometries*. Ph. D. thesis, Imperial College of Science, Technology and Medicine, London.